THE COUPLING OF A DOUBLE QUANTUM DOT TO MICROWAVE PHOTONS

Mohamed Abrash

Department of physics
Lund University

Division: Mathematical physics Lund university
Date: 2022 December the 15th, Duration: 2 months
Supervisors: Peter Samuelsson & Morten Ib Kjærgaard Munk
This thesis is submited for the degree of: Bachelor of science

LUND UNIVERSITY

FACULTY OF SCIENCE

Contents

Abstract

In this study, we derive a mathematical description of a double quantum dot (DQD) embedded in a microwave resonator starting from classical electrostatics. DQDs are a promising platform for building quantum computers and have important applications in quantum sensing and the study of light-matter interactions. Recently, a higher-order sweet spot was discovered, where the DQD is theorized to have improved coherence time. We investigate the coupling strength between the microwave photons and the DQD operating at the higher-order sweet spot, and determine the Rabi frequencies for the case of a strongly driven oscillator in resonance with the DQD energy splitting. This work provides a useful foundation for further research on DQDs and their potential applications in quantum computing and other fields.

Acknowledgments

I am deeply grateful to my supervisors, Peter Samuelsson and Morten I. K. Munk, for providing me with the opportunity to work in their group and for their kind supervision and support throughout my studies.

I would also like to express my sincere thanks to my friends William, Gaurav, Joe, Sebastian, and Alex, for the wonderful time and memories we shared during my studies at Lund University.

Lastly, I am thankful to my parents as well as Julia and Majd, for their unconditional love and support, which has been a constant source of strength and inspiration for me.

Overall, I am grateful to everyone who has contributed to my academic and personal growth during my time at Lund University.

Popular science summary

In the late 1900s, quantum mechanics emerged as one of the most significant breakthroughs in physics. It revolutionized our understanding of the microscopic world, providing insights into the behavior of light, atoms, subatomic particles, and nanoscopic structures. This theory has since become a fundamental part of modern physics and has been the driving force behind many technological advancements. One of the most notable of these advancements is the development of quantum computers, which have the potential to revolutionize various fields such as cybersecurity, weather forecasting, and the simulation of complex molecules. The recognition of the potential of quantum computers has led to a surge in investment by major economic forces, as they seek to harness their powers.

The building blocks of quantum machines are known as quantum bits or qubits. Qubits are the fundamental unit of information used in quantum computers, whereas bits are used in classical computers to store information. Bits are binary units that can be either 0 or 1, while qubits can be in a superposition of 0 and 1 simultaneously, with different probabilities. This superposition, a key feature of quantum physics, gives quantum computers the ability to perform calculations that are difficult to execute on classical computers.

Creating qubits is a real challenge, largely due to the phenomenon of decoherence. This occurs when the tiny particles that make up a quantum computer interact with their environment, causing them to lose their special quantum properties and making them harder to use for quantum computing. To overcome this, scientists are searching for systems that interact less with their environment but can still be controlled and used for quantum computing.

Today, qubits are made in various ways, such as by cooling molecules or atoms using lasers in what is known as trapped ions, or by using superconducting circuits. One of the new methods of making qubits is to use quantum dots. Quantum dots are nanoscopic devices that can be used to trap one or two electrons and harness their quantum properties. Quantum dots can be thought of as small boxes that offer shelter for the electrons, protecting them from decoherence, while still allowing us to influence them by sending microwaves into the dots. In my bachelor's project, I study these systems to understand their mathematical description and to find out if it is possible to influence the electrons in quantum dots using microwaves while providing them with the best protection against decoherence.

Abbreviations

DQD: double quantum dot.
QD: quantum dot.
cQED: circuit quantum electrodynamics.
KCL: Kirchhoff's current law.
KVL: Kirchhoff's voltage law.

Keywords

Quantum computing, Qubit, Double quantum dot (DQD), Microwave resonator, Quantum integrated circuits, Sweet spots, Hybrid quantum circuits.

Tools

The tools used to write this text include Overleaf, Jupyter notebook, Python libraries: Sympy Version 1.10.1, Matplotlib, Numpy.

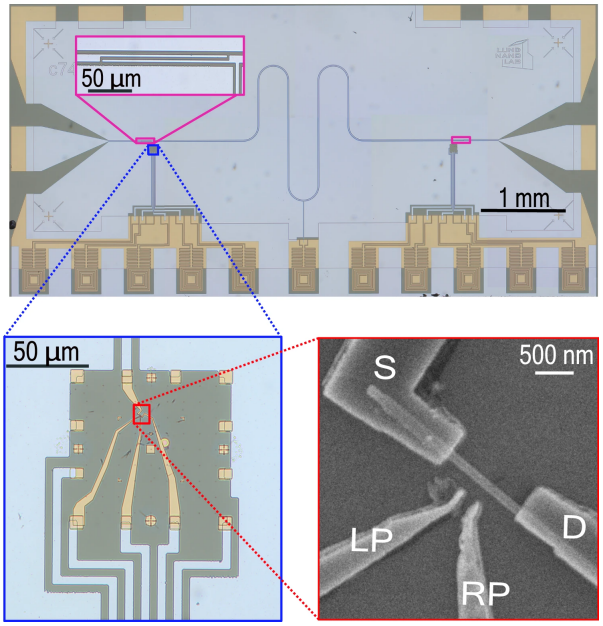

Figure 1: An optical image of a superconducting microwave resonator constructed from aluminum in an integrated circuit is shown in the pink box. Coupled to it is a double quantum dot, which can be seen in the red box. The double quantum dot is integrated into the semiconductor connecting the source S and drain D and is adjusted using left and right gate voltages LP and RP. This setup is used in the field of quantum information and circuit quantum electrodynamics to study the interactions between the electromagnetic waves in the microwave resonator and the electronic states in the double quantum dot. Image source: Khan, W. et al [13]

.

1 Introduction

The development of semiconductor and nanotechnology has enabled us to fabricate various components and circuit elements in the nanoscopic regime, which are controlled by macroscopic parameters such as voltages, currents, and magnetic fields. When these components are isolated from the environment and cooled to low temperatures, quantum phenomena begin to dominate [7]. This has given researchers the ability to construct novel devices that push the boundaries of research and technology. One of the simplest of these devices is the qubit, a two-state/two-level quantum system that can be used in quantum information processing. Theoreticians in the field of quantum computing have explored the potential of realizing qubits and have developed many algorithms that are expected to perform more efficiently on quantum computers. The development of quantum computing technology would enable us to greatly accelerate calculations that are vital to fields such as protein research [16], weather prediction, cybersecurity, artificial intelligence, and more. These calculations are often too complex and time-consuming to be performed on classical computers, but

quantum machines could tackle them with ease, providing significant benefits to society and academia [15].

The study of quantum information theory and algorithms has made significant progress in recent years, but creating physical quantum machines remains a challenge. One of the main obstacles is decoherence, which occurs when quantum states become entangled with the environment or are disrupted by noise. To overcome these issues, researchers have proposed various qubit architectures that are naturally isolated from the environment and more resistant to noise. Despite these advances, the development of reliable, scalable quantum machines is still a work in progress [5, 2].

This bachelor's thesis focuses on the investigation of double quantum dot qubits. A double quantum dot (DQD) is a solid-state device that forms a double well confinement in which electrons can occupy a discrete set of energy levels. [11]. DQD-based qubits can be divided into two categories: spin qubits and charge qubits. The logical space of the qubit is then spanned by the spin of the particles in the DQD or the location of the charge (in one dot or the other). These DQDs can be placed in a microwave resonator, enabling the use of different readout and control protocols [5, 18].

One advantage of charge qubits built using double quantum dots (DQDs) is their ability to be tuned by gate voltages, providing an additional degree of freedom to optimize their performance. By adjusting the parameters of the DQD, it is possible to find a so-called "sweet spot" – a configuration that makes the qubit less susceptible to noise and gives it a longer coherence time. Recently, a new sweet spot for DQDs with two electrons has been proposed, known as the "higher-order sweet spot" [14]. This configuration offers even greater noise resistance and improved coherence time. However, it is not yet clear whether the higher-order sweet spot allows for effective coupling to a microwave resonator, which is the focus of this thesis.

This thesis is structured as follows: we begin with a theoretical section that provides the necessary background knowledge on topics including the mesoscopic limit, double quantum dots, microwave resonators, second quantization, dephasing, and sweet spots. This is followed by a methods section, where we review the techniques from circuit quantum electrodynamics used to derive the quantum mechanical Hamiltonian for quantum circuits. We then apply these methods to find an effective Hamiltonian describing the interaction between a double quantum dot and microwave photons. Finally, we study two interesting cases: one-electron and two-electron double quantum dots. For each case, we diagonalize the double dot Hamiltonian and, by placing the DQD at the sweet spot, we plot the matrix elements of the coupling term to determine if control by microwave photons is possible at the sweet spot.

2 Theory

In this section, we present the necessary background information for studying double quantum dots. This includes the use of second quantization, density matrices, and the introduction of microwave resonators, double quantum dots, and dephasing. These formalisms and concepts will be essential for achieving our research goal of investigating the coupling of double quantum dots to microwave photons at the sweet spot.

2.1 Second quantization

In this thesis, we treat a quantum mechanical system of more than one particle. It is therefore important to understand second quantization; the natural language used to describe many particle quantum physics [1].

A quantum mechanical system that is composed of N identical particles each occupying a state in a Hilbert space $\mathcal{H}_s$, is described by a state in the tensor product space

$$\mathcal{H} = \bigotimes_{i=1}^{N} \mathcal{H}_s = \underbrace{\mathcal{H}_s \otimes \mathcal{H}_s \cdots \otimes \mathcal{H}_s}_{\text{N times}}.$$

In addition to the fundamental quantum mechanics postulates, the state of the system must also adhere to the exchange symmetry postulate; exchanging two indistinguishable particles leaves the state of the system unchanged. Consequently, exchanging two particles leaves in the wave function unchanged for bosons while for fermions it produces a minus sign. One way of implementing the symmetry requirement is to write the system in the language of second quantization where, given a single particle basis $|u_1\rangle, |u_2\rangle, \ldots$, only the number of particles occupying each state matters and we write the state of the N particle system as

$$|n_{u_1}, n_{u_2}, n_{u_3}, \ldots\rangle,$$

where n_{u_i} is the number of particles in state $|u_i\rangle$. Let $\hat{a}_u^\dagger$ and $\hat{a}_u$ be the creation and annihilation operators defined by

$$\begin{aligned} a_{u_i}^\dagger \left|n_{u_i}, n_{u_j}, n_{u_k}, \ldots\right\rangle &= (n_{u_i}+1)^{1/2} \left|n_{u_i}+1, n_{u_j}, n_{u_k}, \ldots\right\rangle, \\ a_{u_i} \left|n_{u_i}, n_{u_j}, n_{u_k}, \ldots\right\rangle &= (n_{u_i})^{1/2} \left|n_{u_i}-1, n_{u_j}, n_{u_k}, \ldots\right\rangle. \end{aligned}$$

The convention being used is that the creation and annihilation operators of a state u_j can only be applied if the number n_{u_j} associated with that state is the first number in the state vector. If this is not the case, then we can permute (or rearrange) the adjacent states in the vector to bring n_{u_j} to the front. However, when working with fermionic states, this permutation will introduce an additional minus sign into the resulting mathematical expression. Using the creation operators, we can generate any quantum state by repeatedly

applying them to the null state and we write

$$\left|n_{u_i}, n_{u_j}, n_{u_k}, \ldots\right\rangle = N \underbrace{a^\dagger_{u_i} a^\dagger_{u_i} \ldots}_{n_{u_i} \text{ times}} \underbrace{a^\dagger_{u_j} a^\dagger_{u_j} \ldots}_{n_{u_j} \text{ times}} a^\dagger_{u_k} \ldots |0\rangle \,,$$

where N is a normalisation constant. Bosonic creation annihilation operators have to satisfy a set of commutation relations to ensure that the exchange symmetry postulate is respected:

$$\begin{aligned} [a^\dagger_{u_j}, a^\dagger_{u_k}] &= 0, & [a_{u_j}, a_{u_k}] &= 0, \\ [a_{u_j}, a^\dagger_{u_k}] &= \delta_{j,k} & &\forall j, k. \end{aligned} \tag{2.1}$$

Likewise, fermionic creation-annihilation operators $c^\dagger$ and c must satisfy the anti-commutation relations

$$\begin{aligned} \{c^\dagger_{u_j}, c^\dagger_{u_k}\} &= 0, & \{c_{u_j}, c_{u,k}\} &= 0, \\ \{c_{u_j}, c^\dagger_{u_k}\} &= \delta_{j,k} & &\forall j, k. \end{aligned} \tag{2.2}$$

Eq. (2.2) dictates that a ferminoic state can only be occupied by 0 or 1 fermions which is a restatement of the Pauli exclusion principle. To simplify the mathematical expressions that describe such states, we adopt the convention of only writing down the occupied states. For example we write

$$|n_{u_1} = 1, n_{u_2} = 0, n_{u_3} = 1\rangle = |u_1, u_3\rangle \,,$$

where it is understood that u_1 and u_3 are occupied by one fermion each while u_2 is not occupied.

2.2 The mesoscopic limit and quantum circuits

In this treatment, we will formally derive and quantize the Hamiltonian governing the dynamics of the double quantum dot and resonator circuit, as shown in Figure 1 and Figure 3. By doing so, we are assuming that this circuit is a quantum integrated circuit. A quantum integrated circuit is a type of electrical circuit that is designed to operate with the collective degrees of freedom of its components being governed by quantum mechanics. This requires two key conditions to be met: superconductivity and low noise.

Superconductivity requires that signals are transported between elements without dissipation. This is an essential requirement to maintain the coherence of the system. The second requirement demands that the circuit and all the wires controlling it are cooled down to low temperatures such that the thermal fluctuations kT are too small to cause any transitions in the circuit. When these conditions are met the circuit is said to be in the mesoscopic regime and its currents and voltages can no longer be considered as classical variables but must be treated as quantum mechanical operators [7, 9].

2.3 Quantum dots

Quantum dots are nanoscopic structures that can accommodate a few electrons. These structures behave like artificial atoms, in the sense that the electrons they host are restricted to a discrete set of energies. The electrons in the quantum dot are confined by a repelling electric potential on all sides [4, p.264]. There are several ways of creating quantum dots, such as by trapping single molecules between electrodes, by using nanowires, by creating semiconducting lateral and vertical dots, and more [10, p.1220].

A double quantum dot (DQD) is created when two dots are coupled by a thin tunneling barrier. The Coulomb interaction between the electrons in the DQD leads to an additional energy cost, called the charging energy, when another electron is added to the DQD. This charging energy can suppress tunneling in and out of the DQD at low temperatures, a phenomenon known as the Coulomb blockade [10, p.1220].

In this thesis, we treat quantum dots using the constant interaction model. This model assumes that the orbital energies of the electrons in the dot are independent of the number of electrons in the dot and that the interactions between the electrons and their environment can be accounted for by a capacitive coupling [10, p.1221]. Additionally, we assume that there are no orbital degrees of freedom in the dots, meaning that we consider the first excitation level to be inaccessible to the electrons.

In this thesis project, we will study double quantum dots in two interesting cases: once when there is only one electron in the DQD, and once when there are two electrons in the DQD.

In the case where only one electron is in the DQD, the basis of the Hilbert space is given by $|L\rangle, |R\rangle$, which are the energy levels in the left and right quantum dots, respectively. The Hamiltonian for this case can be written as:

$$H = E_L c_L^\dagger c_L + E_R c_R^\dagger c_R + t c_R^\dagger c_L + t c_L^\dagger c_R. \tag{2.3}$$

Here, $c_L^\dagger$ and c_L are the creation and annihilation operators for the left quantum dot, $c_R^\dagger$ and c_R are the creation and annihilation operators for the right quantum dot, E_L and E_R are the energies, and t is the tunneling rate between the two dots. In the case of two electrons on the other hand, each electron can be in one of four states, where two additional states are added due to the spin degree of freedom. These four base kets $\{|L,\uparrow\rangle, |L,\downarrow\rangle, |R,\uparrow\rangle, |R,\downarrow\rangle\}$ span the single electron Hamiltonian $\mathcal{H}_e$. The state of the two electron system is then given

by the product space basis :

$$
\begin{aligned}
|L\uparrow\rangle \otimes |R\uparrow\rangle &= c^{\dagger}_{L\uparrow} c^{\dagger}_{R\uparrow} |0\rangle = |u_1\rangle \\
|L\uparrow\rangle \otimes |R\downarrow\rangle &= c^{\dagger}_{L\uparrow} c^{\dagger}_{R\downarrow} |0\rangle = |u_2\rangle \\
|L\downarrow\rangle \otimes |R\uparrow\rangle &= c^{\dagger}_{L\downarrow} c^{\dagger}_{R\uparrow} |0\rangle = |u_3\rangle \\
|L\downarrow\rangle \otimes |R\downarrow\rangle &= c^{\dagger}_{L\downarrow} c^{\dagger}_{R\downarrow} |0\rangle = |u_4\rangle \\
|L\uparrow\rangle \otimes |L\downarrow\rangle &= c^{\dagger}_{L\uparrow} c^{\dagger}_{L\downarrow} |0\rangle = |u_5\rangle \\
|R\uparrow\rangle \otimes |R\downarrow\rangle &= c^{\dagger}_{R\uparrow} c^{\dagger}_{R\downarrow} |0\rangle = |u_6\rangle \,.
\end{aligned} \tag{2.4}
$$

The double quantum dot Hamiltonian can be expressed as:

$$
H = E_C \left(N_L - N_R - n_g\right)^2 + t \sum_{\sigma=\uparrow,\downarrow} \left(c^{\dagger}_{L,\sigma} c_{R,\sigma} + c^{\dagger}_{R,\sigma} c_{L,\sigma} \right), \tag{2.5}
$$

where E_C is the charging energy and t is a tunneling parameter, n_g is a detuning constant while $c^{\dagger}_u$ are fermionic creation operators for a state $|u\rangle$.

2.4 Microwave resonators

Transmission lines or microwave cavities are superconducting waveguides where electromagnetic waves are confined to a two-dimensional structure see Figure 1 and Figure 3. The boundary conditions and geometry of the transmission line limit the electromagnetic waves to a discretised set of modes with set frequencies. It can be shown that the Hamiltonian of a transmission line is found to be the sum of uncoupled harmonic oscillators corresponding to the discretised modes in the cavity:

$$
H = \sum_n \hbar \omega_n a^{\dagger}_n a_n, \tag{2.6}
$$

where $a^{\dagger}_n$ is the creation operator that gives rise to a photon of angular frequency ω_n in the resonator [3]. Within the constant interaction model, coupling between the DQD and a microwave resonator can be modeled capacitivly. Assuming that the microwave resonator is held to low temperatures such that only the ground state excitations are achievable Eq (2.6) simplifies to a single harmonic oscillator. Consequently, a single mode microwave resonator can be modeled by an LC circuit that have the same frequency as the mode since these circuits are known to give rise to quantum mechanical harmonic oscillator once quantised.

Microwave resonators are an essential component of circuit quantum electrodynamics experiments. These resonators allow us to readout and control the state of a double quantum dot. Furthermore, since microwave resonators can isolate a microwave photon with a specific frequency, they offer a powerful tool for studying the interactions between light and matter [18].

2.5 Dephasing and sweet spots

The biggest limiting factor for the implementation of quantum integrated circuits, such as a qubit in a doube quantum dot, is the influence that noise has on the system's state. Random fluctuations in the environment, such as nuclear or charge noise, can lead to undesirable effects such as entanglement with the system or the destruction of our knowledge of it [12]. A simple type of noise that can help us understand dephasing is static noise. For example, consider a two-level system given by the following:

$$H = \frac{\Omega}{2}\sigma_z,$$

where $\pm\frac{\Omega}{2}$ are the energies of the two levels, and σ_z is the pauli z matrix. The effect of static noise can be modeled by adding a constant shift $\xi/2$ to the Hamiltonian, so that it becomes:

$$H = \frac{\Omega + \xi}{2}\sigma_z,$$

Although, this is a simple model, it allows us to study the effects of static noise on the system and devise strategies to combat its impact. Applying the time evolution operator, $\mathcal{U} = e^{-i\frac{(\Omega+\xi)}{2\hbar}\sigma_z t}$ to an initial state $|\psi_0\rangle = \alpha_0 |\downarrow\rangle + \beta_0 |\uparrow\rangle$ yields a state

$$|\psi(t)\rangle = \alpha_0 \exp\left(-i\frac{(\Omega+\xi)t}{2\hbar}\right)|\downarrow\rangle + \beta_0 \exp\left(i\frac{(\Omega+\xi)t}{2\hbar}\right)|\uparrow\rangle\,, \tag{2.7}$$

and the associated density matrix is

$$\rho = \begin{bmatrix} |\alpha_0|^2 & \alpha_0\beta_0^* \exp\left(-i\frac{(\Omega+\xi)}{\hbar}t\right) \\ \alpha_0^*\beta_0 \exp\left(i\frac{(\Omega+\xi)}{\hbar}t\right) & |\beta_0|^2 \end{bmatrix} \tag{2.8}$$

Considering a sample of of such systems where the constant shift ξ takes a random value for each set up. We can find an average density matrix describing the sample by finding the expected value of the off-diagonal elements. Given a random variable ξ that has a probability density $P(\xi)$, the expected value of a function that depends on ξ is defined by

$$\langle f(\xi)\rangle_\xi = \int_{-\infty}^{\infty} d\xi \frac{1}{\sigma\sqrt{2\pi}} \exp\big(-(\xi^2)/2\sigma^2\big) f(\xi).$$

Assuming the noise has a Gaussian probability distribution $N(0,\sigma)$. The expected value of the off-diagonal is then given by

$$\begin{aligned}\langle\rho_{\downarrow,\uparrow}\rangle_\xi &= \alpha_0\beta_0^* \int d(\xi)\frac{1}{\sigma\sqrt{2\pi}} \exp\big(-(\xi^2)/2\sigma^2\big) \exp\left(-i\frac{(\Omega+\xi)}{\hbar}t\right) \\ &= \alpha_0\beta_0^* \exp\left(\frac{-i\Omega t}{\hbar}\right)\exp\left(-(\frac{\xi\sigma t}{\hbar})^2\right).\end{aligned}$$

Thus the effect of static noise is the accumulation of random phase that causes the off diagonal elements of the density matrix to decay as time passes. This means that the expected values of measurements will rapidly tend to the classical values, limiting our ability to observe quantum effects such as superposition which is fundemental for the development of quantum technology. One of the ways one can combat the effect of noise is to look for special choice of parameters that reduces the amplitude of the decay. To sketch how this is done consider again a two level system. However this time, let it be given by:

$$H = \frac{\Omega + \xi}{2}\sigma_z + \Delta\sigma_x. \tag{2.9}$$

where as before ξ is static noise and Δ is a real number. By diagonalizing Eq (2.9), we obtain:

$$H = \frac{\lambda(\xi)}{2}\tilde{\sigma}, \tag{2.10}$$

where $\tilde{\sigma_z}$ is the pauli matrix in the eigenbasis and the eigen energies $\lambda(\xi)$ are given by

$$\lambda = \pm\sqrt{\left(\frac{\Omega + \xi}{2}\right)^2 + \Delta^2}. \tag{2.11}$$

Proceeding as in the first example, the time evolution of the density matrix leads to an offdiagonal phase that depends on the noise. Assuming again that the noise is modeled by a normal distribution $N(0, \sigma)$, we calculate the expected value of the phase:

$$\langle\rho_{\downarrow,\uparrow}\rangle_\xi = \int d(\xi)\frac{1}{\sigma\sqrt{2\pi}}\exp\big(-(\xi^2)/2\sigma^2\big)\exp\left(-i\frac{\lambda(\xi)}{\hbar}t\right). \tag{2.12}$$

Assuming ξ is small, we can approximate the integral by Taylor-expanding λ up to the second order in ξ. We find

$$\begin{aligned}
\langle\rho_{\downarrow,\uparrow}\rangle &= \int d(\xi)\frac{1}{\sigma\sqrt{2\pi}}e^{-(\xi^2)/2\sigma^2}\exp\left(-\frac{it}{\hbar}\left(\lambda_0 + \frac{d\lambda}{d\xi}\xi + \frac{1}{2}\frac{d^2\lambda}{d\xi^2}\xi^2\right)\right) \\
&= \exp\left(\frac{1}{2}\left(\log\Big(1 - it\sigma^2\lambda^{''}\Big) - \log\Big(1 + t^2\sigma^4\lambda^{''2}\Big)\right) - \frac{t^2\sigma^2\lambda^{'2}}{2 + 2it\sigma^2\lambda^{''}}\right) \\
&\approx \exp(-it\lambda_0/\hbar)\exp\left(-\frac{1}{2}it\sigma^2\lambda^{''}\right)\exp\left(-\frac{1}{2}t^2\sigma^4\lambda^{''2} - \frac{1}{2}t^2\sigma^2\lambda^{'2}\right).
\end{aligned}$$

Thus again, we find that the off-diagonal elements decay with $\exp\big(-\frac{1}{2}\Gamma t^2\big)$, where the decay rate Γ is given by

$$\Gamma \approx \lambda^{'2}\sigma^2 + \lambda^{''2}\sigma^4 \tag{2.13}$$

This equation shows that the rate at which a quantum system decoheres can be slowed down by minimizing the eigenvalues in terms of the noise that is affecting the system. The point at which the first derevative is zero ($d\lambda/d\xi = 0$), is called the sweet spot. Generally as discussed in [14], an n'th order sweet spot is found by setting $d^k\lambda/d\xi^k = 0$ for all $k \leq n$.

3 Method

The traditional approach to electrical circuits involves using Maxwell's or Kirchhoff's laws to explain circuit behavior. However, this method fails for quantum circuits in the mesoscopic limit where voltages and currents must be treated as non-commutative quantum operators [8, 9]. To accurately describe these systems, a quantization of the equations of motion is required. In this section, the method of circuit quantum electrodynamics (cQED) is discussed as a way to obtain a quantum description of super-conducting circuits in the quantum limit by transforming classical laws into a quantum formalism. Despite its promise, this method has limitations, as it may overlook important quantum phenomena. For example, the tunneling of electrons between dots in a double quantum dot-microwave resonator is not considered. The section first reviews the classical treatment of circuits, then introduces definitions necessary for a Lagrangian formalism, and finally outlines the quantization process for non-dissipative circuits as developed in [6].

3.1 Branch variables

The current and voltage across an electrical element or branch are classically defined as:

$$v_b(t) = \int_{\text{start}}^{end} \vec{E}.d\vec{l},$$

$$i_b(t) = \int_S \vec{B} \cdot d\vec{S}, \tag{3.1}$$

where the voltage v_b integrates the electric field E over an arbitrary simple line connecting the start and end of the element while the current i_b is the integral of the magnetic field B over a Gaussian surface S containing the element. An arbitrary orientation is assigned to each element which further induces a sign for the current and voltage as seen in figure 2 .

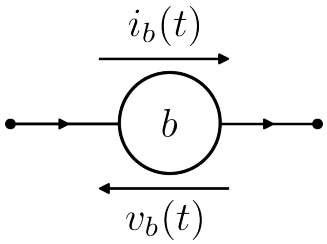

Figure 2: According to the typical sign convention for electric circuits, the current i_b and voltage v_b of a branch (b) are defined as follows: the direction of the current is taken to be the same as the direction of the branch, with the current flowing into the positive terminal of the branch. The voltage is then defined as the potential difference between the positive and negative terminals of the branch, with the voltage taken as the electric potential at the positive terminal minus the electric potential at the negative terminal. In this way, the direction of the branch is defined to be the same as the direction of the current flowing through it.

Any valid electrical circuit must obey two physical constraints known as Kirchhoff's law. The first, Kirchhoff's current law (KCL), is given by

$$\sum_k i_k = 0, \tag{3.2}$$

where the summation runs over every branch k connected to a given node (a junction between elements). This law reflects the conservation of charge in the circuit; the sum of all currents going to a node must equal the sum of the current leaving it. The other constraint is Kirchhoff's voltage law (KVL) given by:

$$\sum_{i \in l} v_i = 0. \tag{3.3}$$

The sum of branch voltages around a closed loop (l) must be zero. This law casts the irrational/conservative nature of the electric field into a form that is convenient for circuit analysis.

3.2 Capacitive and inductive elements

Circuit elements can be classified into capacitve elements that satisfy $v_b = f(Q_b)$ for some function $f(.)$ and inductive elements that satisfy $i = g(\Phi)$ for some $g(.)$ where Q_b and Φ are the branch charge and voltage flux and are defined as the time integrals of the current and voltage respectively:

$$Q_b(t) = \int_0^t i_b(\tau) d\tau \tag{3.4}$$

$$\Phi_b(t) = \int_0^t v_b(\tau) d\tau. \tag{3.5}$$

In addition to relating the voltages and currents of capacitive and inductive elements, flux and charge variables prove to be very useful since they allow us to cast Kirchhoff's laws into a second order differential equations in time which we can integrate to get a Lagrangian for the system. For the scope of this thesis we limit ourselves to linear elements. This means that the functions $f(.)$ and $g(.)$ have to be linear in Q_b and Φ_b and the conventional capacitor and inductor relations are regained:

$$v_b = \frac{Q_b}{C}, \tag{3.6}$$

and

$$i_b = \frac{\phi_b}{L}, \tag{3.7}$$

where C and L are the capacitance and inductance respectively. It will also be useful - given that we want to work with a Lagrangian and Hamiltonian formalism- to see what the energy stored in a these elements look like.

The energy of an electrical element is found by integrating the power $p_b = i_b v_b$ over time. For a linear capacitor with capacitance C we have :

$$E_b = \int i_b v_b dt = \int \frac{Q_b i_b}{C} dt = \int \frac{Q_b \cdot \frac{dQ_b}{dt}}{C} dt = \frac{Q_b^2}{2C}. \tag{3.8}$$

Similarly for inductive elements

$$E_b = \int \frac{d\Phi_b}{dt} \cdot \frac{\Phi_b}{L} dt = \frac{\Phi_b^2}{2L}. \tag{3.9}$$

3.3 Node variables and Lagrangian formalism

In light of the previous definitions, a circuit of N elements is described by as many as $2N$ variables: a branch flux Φ and branch charge Q for every single element in the circuit. However, since Kirchhoff's laws introduce two constraints, the variables we defined thus far cannot be generally independent. This problem is commonly resolved by using the node variable method where we define one node as a reference node and then define the flux at any other node (n) as the sum of all voltage fluxes between the ground and node (n), formally we define

$$\phi_n(t) = \int_0^t d\tau \int_{\text{ground}}^n \vec{E} \cdot \vec{dl}, \tag{3.10}$$

or equivalently, in terms of branch variables:

$$\phi_n(t) = \sum_{m \in p} (-1)^S \Phi_m(t), \tag{3.11}$$

where p is any path in the circuit that starts at the ground node and ends at node n. Meanwhile S is a parameter ensuring that the summation adds up to the integral in Eq. (3.10). $S = 2$ if the branch is oriented along p and $S = 1$ otherwise. With this definition, the voltage across an element is given by

$$v_b(t) = \dot{\phi}_n(t) - \dot{\phi}_m(t), \tag{3.12}$$

where (n) is the node at the end of the element and (m) is the node at the beginning (note the relevance of the branch orientation).

The introduction of node variables has two desired outcomes. Firstly, node fluxes are independent and our variables automatically satisfy KVL. Secondly, we can now relate the dynamics of the system directly into node variables. We will shortly see that this provides a natural way to describe a system where we model a quantum dot as the node in the circuit.

3.4 General scheme for obtaining the Hamiltonian

Having defined all the necessary variables we now turn to the algorithm explained in detail by M.Devoret [6] for obtaining the Hamiltonian of a non-dissipating superconducting circuits. The following procedure will be used to obtain the Hamiltonian of the equivalent circuit model of a DQD in a microwave resonator:

- Choose an orientation for all the elements
- Pick a reference node
- Express voltages in terms of node fluxes
- Write KCL for each node
- Obtain the Euler-Lagrange equations by integrating KCLs
- Perform a Legendre transformation to get a the Hamiltonian
- Quantise the Hamiltonian by replacing classical variables by algebraic operators and the Poisson brackets by commutators.

For an illustrative example see the appendix.

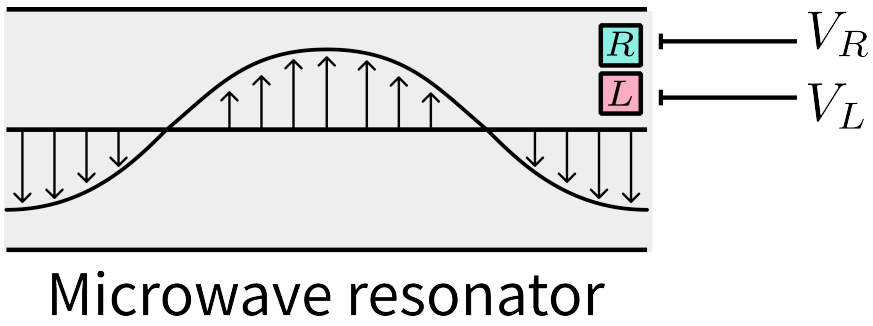

Figure 3: A schematic of a microwave resonator hosting a double quantum dot where L and R stand for left quantum dot, and right quantum dot respectively. By fixing the boundary conditions of the microwave resonators, the electromagnetic waves in the resonator are restricted to a specific set of frequencies called the resonator's modes. Absorption or emission of the microwave modes by the double quantum dot happen when an energy transition in the DQD matches the frequency of a resonator's mode.

4 Deriving the Hamiltonian

In this section, we will show how to derive the Hamiltonian that describes the dynamics of a double quantum dot inside a microwave resonator. We will begin by creating a circuit model of the setup shown in Figure 3. Next, using the method outlined in Section 3, we will find the classical Hamiltonian of the circuit. Finally, we will use two steps to quantize the Hamiltonian. First, we will introduce fermionic operators, and then we will quantize the bosonic part.

4.1 Equivalent circuit

In this section, we will model the microwave resonator and double quantum dot (DQD) shown in Figure 1 using a simple circuit model that allows us to apply the laws of electrostatics to the system. A simplified version of the setup is shown in Figure 3. Based on our discussions in Section 2.4 and Section 2.3, we can replace the microwave resonator with an LC circuit that has the same fundamental frequency. Additionally, we will assume that the LC circuit is capacitively coupled to the DQD. We will model the charge confined to a quantum dot as the charge on the connection between two capacitors. Furthermore, we will include a capacitive coupling between the dots to take into account the Coulomb interaction between them.

Figure 4 shows an equivalent circuit model for the full setup where the charge on the nodes n_R and n_L correspond to the charges on the right and left quantum dot respectively. C_R and C_L account for the coupling to the microwave mode while C_{Rg} and C_{Lg} are capacitive couplings to gate electrodes that can be used to tune the DQD. The electrodes allow us to change the boundary conditions of the circuit by controlling the potentials V_R and V_L.

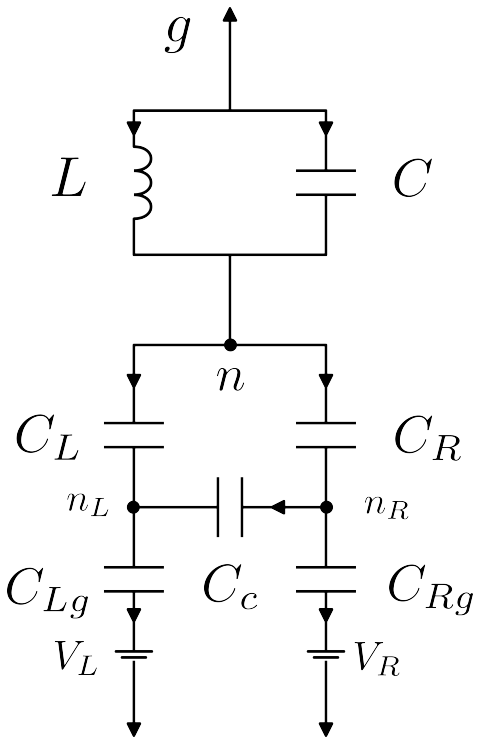

Figure 4: The circuit equivalence to a double quantum dot placed inside a microwave resonator. The charge in the double quantum dot is equal to the charge on the nodes n_R and n_L and the LC circuit models microwave photons with frequency $\omega = 1/\sqrt{LC}$. The double quantum dot is coupled capacitivly to the LC circuit through C_L and C_R. Gate voltages V_L and V_R are used to tune the double dot. g is the ground node.

4.2 The classical Hamiltonian

Following the algorithm at the end of Sec 3, an orientation is chosen for every element of the circuit model as one can see in figure 4. Node fluxes $\phi_n, \phi_{n_L}, \phi_{n_R}$ are defined by Eq. (3.11). Currents and voltages across elements are expressed in terms of flux variables by employing Eq (3.7), Eq. (3.6) and Eq. (3.12) and we obtain the following expressions:

$$
\begin{aligned}
i_C &= \dot{V}_C C = C\ddot{\phi}_n \\
i_{C_R} &= \dot{V}_{C_R} C_R = C_R(\ddot{\phi}_{n_R} - \ddot{\phi}_n) \\
i_{C_L} &= \dot{V}_{C_L} C_L = C_R(\ddot{\phi}_{n_L} - \ddot{\phi}_n) \\
i_{C_C} &= \dot{V}_{C_C} C_C = C_C(\ddot{\phi}_{n_L} - \ddot{\phi}_{n_R}) \\
i_{C_{Rg}} &= \dot{V}_{C_{Rg}} C_{Rg} = C_{Rg}(\dot{V}_R - \ddot{\phi}_{n_R}) \\
i_{C_{Lg}} &= \dot{V}_{C_{Lg}} C_{Lg} = C_{Lg}(\dot{V}_L - \ddot{\phi}_{n_L}) \\
i_L &= \frac{\phi_n}{L},
\end{aligned}
$$

where V_E and i_E are the voltage and current across an element E, while ϕ_m is the node flux at a junction m as defined in Eq. (3.5). KCL can now be written in terms of flux variables: At node n as

$$C\ddot{\phi}_n + \frac{\phi_n}{L} = C_R(\ddot{\phi}_{nR} - \ddot{\phi}_n) + C_L(\ddot{\phi}_{nL} - \ddot{\phi}_n),$$

at node n_R

$$C_R(\ddot{\phi}_{nR} - \ddot{\phi}_n) = C_{gR}(V_R - \ddot{\phi}_{nR}) + C_c(\ddot{\phi}_{nL} - \ddot{\phi}_{nR}),$$

and at n_L as

$$C_L(\ddot{\phi}_{nL} - \ddot{\phi}_n) + C_C(\ddot{\phi}_{nL} - \ddot{\phi}_{nR}) = C_{gL}(\dot{V}_L - \ddot{\phi}_{nL}).$$

These relations can be taken to be the Euler-Lagrange equations satisfying

$$\frac{d}{dt}\frac{\partial \mathcal{L}}{\partial \dot{\phi}_m} = \frac{\partial \mathcal{L}}{\partial \phi_m}, \forall m \in \{n_R, n_L, n\}, \tag{4.1}$$

for the following Lagrangian

$$\mathcal{L} = \frac{C\dot{\phi}^2}{2} - \frac{\phi_n^2}{2L} + \frac{C_R(\dot{\phi}_R - \dot{\phi}_n)^2}{2} + \frac{C_{RG}(V_R - \dot{\phi}_R)^2}{2} + \frac{C_L(\dot{\phi}_L - \dot{\phi}_n)^2}{2} + \frac{C_{LG}(V_L - \dot{\phi}_L)^2}{2} + \frac{C_C(\dot{\phi}_L - \dot{\phi}_R)^2}{2}. \tag{4.2}$$

Comparing to Eq. (3.8) and Eq. (3.9) we see that the Lagrangian is given as the energy difference between the capacitive and inductive elements. That is, energy stored in the electric field of the capacitors and energy stored in the magnetic field of the inductors, play the same role that kinetic and potential energy play in classical mechanics. The generalised momenta of the voltage fluxes are defined by

$$Q_m = \frac{\partial \mathcal{L}}{\partial \dot{\phi}_m}, \forall m \in \{n_R, n_L, n\}. \tag{4.3}$$

Carrying out the calculations for $\phi_n\phi_L, \phi_R$ gives:

$$\begin{aligned} Q_n &= C\dot{\phi}_n + C_L(\dot{\phi}_n - \dot{\phi}_L) + C_R(\dot{\phi}_n - \dot{\phi}_R) \\ Q_R &= C_R(\dot{\phi}_R - \dot{\phi}_n) + C_C(\dot{\phi}_R - \dot{\phi}_L) + C_{Rg}(\dot{\phi}_R - V_R) \\ Q_L &= C_L(\dot{\phi}_L - \dot{\phi}_n) + C_C(\dot{\phi}_L - \dot{\phi}_R) + C_{Lg}(\dot{\phi}_L - V_L). \end{aligned} \tag{4.4}$$

Note that the conjugate momenta in this case correspond to the charges on the nodes. This can be seen by observing that $(Q_{nR} = Q_R - Q_C - Q_{RG})$. This is a very important feature of our circuit model. The dynamical variables describing our system are directly related to the node charges. This allows us to take Q_R as the charge on the right quantum dot, and Q_L as the charge on the left one.

Now that we have found the Lagrangian and conjugate momenta that describe the system, we can use a Legendre transformation to obtain a Hamiltonian expression. This involves inverting Eq. (4.4). It is easiest to do this by first writing the equations in matrix form and then finding the inverse matrix. Thus, define

$$\vec{q} = \begin{bmatrix} Q_n \\ Q_{nR} + V_R C_{gR} \\ Q_{nL} + V_L C_{gL} \end{bmatrix}, \dot{\vec{\phi}} = \begin{bmatrix} \dot{\phi}_n \\ \dot{\phi}_R \\ \dot{\phi}_L \end{bmatrix}, \tag{4.5}$$

and

$$C = \begin{bmatrix} C_L + C + C_R & -C_R & -C_L \\ -C_R & C_C + C_R + C_{gR} & -C_C \\ -C_L & -C_C & C_C + C_L + C_{gL} \end{bmatrix}. \tag{4.6}$$

With these definitions, Eq. (4.4) becomes

$$\vec{q} = C \cdot \dot{\vec{\phi}}, \tag{4.7}$$

and its inverse is $\dot{\vec{\phi}} = C^{-1} \cdot \bar{q}$. Before performing the transformation, it is useful to factorise the Lagrangian and write it as

$$\mathcal{L} = \frac{Q_n\dot{\phi}_n}{2} + \frac{(Q_L - C_{Lg}V_L)\dot{\phi}_L}{2} + \frac{(Q_R - C_{Rg}V_R)\dot{\phi}_R}{2} - \frac{\phi_n^2}{2L}.$$

It is easy now to see that the Hamiltonian is given by

$$H = \sum Q_m\dot{\phi}_m - \mathcal{L} = \frac{Q_n\phi_n}{2} + \frac{(Q_R + C_{Rg}V_R)\dot{\phi}_R}{2} + \frac{(Q_L + C_{Lg}V_L)\dot{\phi}_L}{2} + \frac{\phi_n^2}{2L}.$$

Finally, we complete the transformation by substituting the inverse relation of Eq. (4.7), giving us:

$$H = \vec{q}^T \cdot (C^{-1}) \cdot \vec{q} + \frac{\phi_n^2}{2L}. \tag{4.8}$$

Expanding this expression and defining $M_{i,j} = [(C^{-1})]_{i,j}$, we arrive at

$$\begin{aligned} H =& \frac{1}{2}M_{11}Q_n^2 + \frac{1}{2}M_{22}Q_R^2 + \frac{1}{2}M_{33}Q_L^2 \\ &+ Q_L[C_{gL}M_{33}V_L + C_{gR}V_R M_{23}] \\ &+ Q_R[C_{gL}V_L M_{23} + C_{gR}M_{22}V_R] \\ &+ Q_n[C_{gL}V_L M_{13} + C_{gR}V_R M_{12}] \\ &+ Q_n[Q_L M_{13} + Q_R M_{12}] \\ &+ Q_R Q_L M_{23} \\ &+ \frac{\phi_n^2}{2L}. \end{aligned}$$

Renaming the constant coefficients, we obtain the following classical Hamiltonian of the circuit shown in Figure 4:

$$H = \frac{1}{2}\alpha_n Q_n^2 + \alpha_R \frac{1}{2}Q_R^2 + \frac{1}{2}\alpha_L Q_L^2 + \beta_L Q_L + \beta_R Q_R + \beta_n Q_n + Q_n(\gamma_L Q_L + \gamma_R Q_R) + \delta Q_L Q_R + \frac{\phi_n^2}{2L}. \tag{4.9}$$

4.3 Introducing Fermionic operators and the tunneling term

The Hamiltonian derived in Eq. (4.9) is cyclic in ϕ_R and ϕ_L which reflects the conservation of node charges. However, we are interested in studying a system of two quantum dots that are only separated by a thin barrier allowing the electrons to tunnel from one dot to the other. Since this phenomenon is intrinsically quantum mechanical, we do not expect our classical model to reproduce it and it is not possible to add a circuit element to take it into account. Therefore, a tunneling term H_t should be added to the Hamiltonian. This will break the conservation of charge on each quantum dot, but it does preserve the total charge $Q_L + Q_R$. As a result, we can rewrite the Hamiltonian in a form that reflects this conservation. We therefore collect and factorise the Q_L and Q_R terms such that the Hamiltonian only contains $Q_L + Q_R$ and $(Q_L - Q_R)$ terms. This is done in two steps first in this section we factorise the Q_n coefficients and introduce the fermionic operators and then we deal with the uncoupled Q_R and Q_L terms in the algebraic treatment section.

Factorising the Q_n coefficients :

$$\begin{aligned} H =& \frac{1}{2}\alpha_n Q_n^2 + \frac{Q_n}{2}((\gamma_L + \gamma_R)(Q_L + Q_R) + (\gamma_L - \gamma_R)(Q_L - Q_R)) + \beta_n Q_n + \frac{\phi_n^2}{2L} \\ &+ \alpha_R \frac{1}{2}Q_R^2 + \frac{1}{2}\alpha_L Q_L^2 + \beta_L Q_L + \beta_R Q_R + \delta Q_L Q_R + H_t. \end{aligned} \tag{4.10}$$

In the mesoscopic limit of the DQD circuit, we must reintroduce the charge variables as quantum mechanical operators counting the number of electrons in each dot and we write

$$\begin{aligned} Q_L &\to \widehat{Q}_L = e\widehat{N}_L \\ Q_R &\to \widehat{Q}_R = e\widehat{N}_R, \end{aligned} \tag{4.11}$$

where e is the electron charge and $\hat{N}$ is a number operator. Furthermore, we assume that the electrons in the dot have no orbital degrees of freedom and are therefore confined to only two states: spin up and spin down. In second quantization language, an electron in the left quantum dot can be in one of two states

$$\begin{aligned} |L,\uparrow\rangle &= c^\dagger_{L,\uparrow}|0\rangle\,, \\ \text{or } |L,\downarrow\rangle &= c^\dagger_{L,\downarrow}|0\rangle\,, \end{aligned} \tag{4.12}$$

and $c^\dagger$,c are fermionic operators satisfying the anti-commutation relations (2.2). The number operators $\widehat{N}_L$ counts the electrons present in both states:

$$\widehat{N}_L = c^\dagger_{L,\uparrow}c_{L,\uparrow} + c^\dagger_{L,\downarrow}c_{L,\downarrow}. \tag{4.13}$$

The conservation of total charge can now be expressed as $Q_L + Q_R = eN$ for a fixed number of electrons N. This constraint allows us to eliminate Q_R from the equations by writing

$$Q_L - Q_R = 2e\hat{N}_L - 2e\frac{N}{2}. \tag{4.14}$$

Furthermore, the tunneling term can be written on the form:

$$H_t = t\sum_{\sigma=\uparrow,\downarrow} c^\dagger_{L,\sigma}c_{R,\sigma} + c^\dagger_{R,\sigma}c_{L,\sigma}, \tag{4.15}$$

where t is some real constant that depends on the architecture of the double quantum dot. Implementing all the changes that we have introduced so far, we find:

$$\begin{aligned} H =& \frac{1}{2}\alpha_n Q_n^2 + \gamma_- e\widehat{N}_L Q_n + \left(\beta_n + e\frac{N}{2}\gamma_+ - e\frac{N}{2}\gamma_-\right)Q_n + \frac{\phi_n^2}{2L} \\ &+ \alpha_R\frac{1}{2}\widehat{Q}_R^2 + \frac{1}{2}\alpha_L\widehat{Q}_L^2 + \beta_L\widehat{Q}_L + \beta_R\widehat{Q}_R + \delta\widehat{Q}_L\widehat{Q}_R \\ &+ H_t. \end{aligned} \tag{4.16}$$

We will soon see that this expression is composed of three parts, a double quantum dot term, a harmonic oscillator term and a coupling term mixing the two. However to see that we must first quantize the harmonic oscillator.

4.4 Quantization of the Harmonic oscillator

Inspecting the Poisson's brackets of ϕ_n and Q_n we find that $\{\phi_n, Q_n\} = 1$ where ϕ_n is taken as the main coordinate. Consequently, the dynamics of the ϕ_n are that of a harmonic oscillator. Furthermore, it is useful to note that for a harmonic oscillator, the equations of motion are invariant under the exchange of the roles of ϕ_n and Q_n [9, p.124]. Since it is more useful to us, we will regard Q as the coordinate and ϕ as the momentum while keeping $\{Q_n, \phi_n\} = 1$.

The quantum mechanical description of the LC circuit can now be found by carrying out a canonical quantization where we set:

$$[\widehat{Q}_n, \widehat{\phi}_n] = i\hbar\{Q_n, \phi_n\} = i\hbar. \tag{4.17}$$

Following the typical treatment of harmonic oscillators we factorize the Hamiltonian by defining the ladder operators a and $a^\dagger$ as

$$\begin{aligned} a &= \sqrt{\frac{\alpha_n}{2\hbar w}}\widehat{Q} + i\frac{1}{\sqrt{2\hbar L w}}\widehat{\Phi}, \\ a^\dagger &= \sqrt{\frac{\alpha_n}{2\hbar w}}\widehat{Q} - i\frac{1}{\sqrt{2\hbar L w}}\widehat{\Phi}, \end{aligned} \tag{4.18}$$

where $\omega^2 = \frac{\alpha_n}{L}$ and a,$a^\dagger$ are bosonic creation-annihilation operators satisfying the bosonic commutation relations Eq. (2.1). Consequently, the operator $a^\dagger$ creates a photon in the circuit with angular frequency ω while a removes one. By inverting Eq. (4.18), we also find

$$\widehat{Q} = \frac{\sqrt{2\hbar\omega}}{2\sqrt{\alpha_n}}(a + a^\dagger) = \hbar(4\hbar^2 L\alpha_n)^{-1/4}(a^\dagger + a). \tag{4.19}$$

Moreover, we introduce the following constants:

$$\begin{aligned} \omega_Q &= e\cdot\gamma_-(4\hbar^2 L\alpha_n)^{-1/4} \\ \omega_o &= \left(\beta_n + e\frac{N}{2}\gamma_+ - e\frac{N}{2}\gamma_-\right)\left(4\hbar^2 L\alpha_n\right)^{-1/4}. \end{aligned} \tag{4.20}$$

The Hamiltonian becomes:

$$\begin{aligned} H =& \hbar\omega\left(a^\dagger a + \frac{1}{2}\right) + \hbar\omega_Q\left(a^\dagger + a\right)\widehat{N}_L + \hbar\omega_o\left(a^\dagger + a\right) \\ &+ \alpha_R\frac{1}{2}\widehat{Q}_R^2 + \frac{1}{2}\alpha_L\widehat{Q}_L^2 + \beta_L\widehat{Q}_L + \beta_R\widehat{Q}_R + \delta\widehat{Q}_L\widehat{Q}_R \\ &+ H_t. \end{aligned} \tag{4.21}$$

The first term corresponds to a harmonic oscillator while the second term stands for the coupling between the photons and the double quantum dot. Another important term that our derivation has produced is a term proportional to $(a^\dagger + a)$. This term does not contribute to the dynamics and only results in a shift in the harmonic oscillator's energies which can be seen by defining new operators $\alpha = a + \frac{\omega_0}{\omega}$ and noting that α and $\alpha^\dagger$ still satisfy the bosonic commutation relations Eq. (2.1). Consequently the Hamiltonian can be expressed in these operators as

$$\begin{aligned} H =& \hbar\omega\left(\alpha^\dagger\alpha + \frac{1}{2} - \frac{\omega_o^2}{\omega^2}\right) + \hbar\omega_Q\left(\alpha^\dagger + \alpha - \frac{2\omega_o}{\omega}\right)\widehat{N}_L \\ &+ \alpha_R\frac{1}{2}Q_R^2 + \frac{1}{2}\alpha_L Q_L^2 + \beta_L Q_L + \beta_R Q_R + \delta Q_L Q_R + H_t. \end{aligned} \tag{4.22}$$

To this point, we are able to discern three different terms and the Hamiltonian is separated into

$$H = H_{HO} + H_C + H_{DQD}, \tag{4.23}$$

where H_{HO}, H_C, H_{DQD} are the harmonic oscillator Hamiltonian, the coupling term and the double dot Hamiltonian defined by

$$H_{HO} = \hbar\omega \left(\alpha^\dagger \alpha + \frac{1}{2} - \frac{\omega_o^2}{\omega^2}\right) \tag{4.24}$$

$$H_C = \hbar\omega_Q \hat{N}_L \left(\alpha^\dagger + \alpha\right) \tag{4.25}$$

$$H_{DQD} = \alpha_R \frac{1}{2}\widehat{Q}_R^2 + \frac{1}{2}\alpha_L \widehat{Q}_L^2 + \beta_L^{'}\widehat{Q}_L + \beta_R \widehat{Q}_R + \delta \widehat{Q}_L \widehat{Q}_R + H_t, \tag{4.26}$$

where we defined $\beta_L^{'} = \beta_L - \left(\frac{2\hbar\omega_Q\omega_o}{e\omega}\right)$.

4.5 Algebraic treatment of the double quantum dot Hamiltonian

The double quantum dot expression Eq. (4.26) can be further simplified by reinstating the total charge conservation and rewriting it in the following form:

$$H_{DQD} = A\left(Q_L + Q_R - N_g\right)^2 + B\left(kQ_L - \frac{Q_R}{k} - n_g\right)^2 + H_t, \tag{4.27}$$

for some constants A, B, k, n_g and N_g. To find these constants in terms of the old ones, we can expand Eq. (4.27) and equate it to Eq. (4.26). Finding the new constants A, B, k, N_g, n_g is then equivalent to solving the following system of nonlinear equations:

$$\begin{aligned}
&\frac{\alpha_L}{2} = A + Bk^2, \\
&\frac{\alpha_R}{2} = A + \frac{B}{k^2}, \\
&\delta = 2A - 2B, \\
&\beta_R = -2AN_g + \frac{2Bn_g}{k}, \\
&\beta_L^{'} = -2AN_g - 2Bkn_g.
\end{aligned} \tag{4.28}$$

The solutions to this system of equations are found in Appendix. Note that the relation $[\widehat{Q}_L, \widehat{Q}_R] = 0$ has been used.

Finally, using second quantization and the conservation of total charge Eq. (4.14), we express the second term of Eq. (4.27) as:

$$B\left(ke\widehat{N}_L - \frac{e\widehat{N}_R}{k} - n_g\right)^2 = B\left(ke\widehat{N}_L + \frac{e\widehat{N}_L}{k} - n_g - \frac{eN}{k}\right)$$
$$= E_C(\widehat{N}_L - n)^2.$$

Given that the constants E_C and n are defined as

$$E_C = Be^2(k + \frac{1}{k})^2, \tag{4.29}$$

$$n = \frac{\frac{n_g}{e} + \frac{N}{k}}{k + \frac{1}{k}}. \tag{4.30}$$

The double quantum dot H_{DQD} is now rewritten as:

$$H_{DQD} = E_C(\widehat{N}_L - n)^2 + H_t. \tag{4.31}$$

Note for the Hamiltonian of a double quantum dot written on the form of Eq. (4.31) the first order sweet spot is at $n = \frac{N}{2}$, and the higher order sweet spot for $N = 2$ is at $n = 1$ and $E_C/t = (6\sqrt(2) - 8)^{1/2}$ [14]. Plugging the double quantum dot Hamiltonian back into Eq. (4.23), we find

$$H = \hbar\omega\left(\alpha^\dagger\alpha + \frac{1}{2} - \frac{\omega_o^2}{\omega^2}\right) + \hbar\omega_Q\hat{N}_L\left(\alpha^\dagger + \alpha\right) + E_C\left(\widehat{N}_L - n\right)^2 + t\sum_{\sigma=\uparrow,\downarrow} C^\dagger_{L,\sigma}C_{R,\sigma} + C^\dagger_{R,\sigma}C_{L,\sigma}. \tag{4.32}$$

This equation is a key finding of the thesis. It describes the Hamiltonian of a double quantum dot interacting with microwave photons. The constants in the equation are determined by the capacitances shown in Figure 4. With this equation, we can investigate the dynamics of the system in the presence of various sources of noise and dissipation, and study the different operations that can be performed on the double quantum dot using the microwave resonator

4.6 Weak coupling limit

We found that the Hamiltonian of the double quantum dot in a microwave resonator is given by Eq. (4.32) where all the constants appearing in the equation are defined in terms of various circuit capacitances except for t (the tunneling constant) which depends on the manufacturing of the quantum dots. Since the DQD interacts with the microwave resonator only through the capacitancies C_L and C_R, we expect that when these capacitances are small, the coupling to the microwave resonator vanishes. In this limit the coupling constant must go to zero and the frequency of the LC circuit must decouple and become independent of the rest of the circuit.

This limit can be found by introducing two parameters ϵ_L and ϵ_R and letting

$$C_L \longrightarrow \frac{C_L}{C} C \coloneqq \epsilon_L C, \tag{4.33}$$

$$\text{and } C_R \longrightarrow \frac{C_R}{C} C \coloneqq \epsilon_R C, \tag{4.34}$$

where ϵ_L and ϵ_R quantify the magnitude of C_L and C_R with respect to C. Expressing all of the constants in terms of ϵ_L, ϵ_R and taking the limit as $\epsilon_L, \epsilon_R \longrightarrow 0$, we get:

$$H^{(0)} = \frac{1}{\sqrt{LC}} \hbar \left(a^\dagger a + \frac{1}{2} \right) + E_C^{(0)} \left(\widehat{N}_L - n^{(0)} \right)^2 + t \sum_{\sigma=\uparrow,\downarrow} C_{L,\sigma}^\dagger C_{R,\sigma} + C_{R,\sigma}^\dagger C_{L,\sigma} \tag{4.35}$$

As expected this limit gives a Hamiltonian describing an isolated harmonic oscillator and a DQD with no terms mixing the two. The angular frequecy of the LC oscillator tends to the uncoupled value of $\frac{1}{\sqrt{LC}}$. The charging energy and detuning of the DQD tend to the constants $E_C^{(0)}$ and $n^{(0)}$ that are independent of the LC circuit. Although, in this text, this limit serves merely as a sanity check, it also tells us that the coupling term $\hbar\omega_Q \widehat{N}_L (a + a^\dagger)$ may be included as a small perturbation added to Eq. (4.35) if the coupling capacitances C_L and C_R are made small enough. The leading contribution to the coupling constant is given by

$$\omega_Q = \frac{e\left(-C_{Lg}\epsilon_r + C_{Rg}\epsilon_l\right)}{\left(\frac{4\hbar^2 L}{C}\right)^{0.25} \left(C_C C_{Lg} + C_C C_{Rg} + C_{Lg} C_{Rg}\right)}, \tag{4.36}$$

where e is the electron charge and the capacitencies are defined in Eq. (4.6).

5 Matrix elements of the coupling term

In this section, we aim to determine if it is possible for the microwave photons to couple with the double quantum dot at the higher-order sweet spot. Our approach is to first diagonalize the Hamiltonian of the double quantum dot and then express the coupling term in the resulting eigenbasis.

5.1 One Electron Double Quantum Dot

In the case where there is only 1 electron in the DQD. The Hilbert space of the DQD is panned by the electron orbitals in the left and right dot; $|L\rangle$ and $|R\rangle$, and the Hamiltonian Eq. (4.31) simplifies to :

$$H_{DQD} = E_C \left(\hat{C}_L^\dagger \hat{C}_L - n\right)^2 + tC_L^\dagger C_R + tC_R^\dagger C_L. \tag{5.1}$$

In matrix form this is given by:

$$H_{DQD} \longrightarrow \begin{bmatrix} \langle L| H_{DQD} |L\rangle & \langle L| H_{DQD} |R\rangle \\ \langle R| H_{DQD} |L\rangle & \langle R| H_{DQD} |R\rangle \end{bmatrix} = \begin{bmatrix} E_C(1-n)^2 & t \\ t & E_C n^2 \end{bmatrix}. \tag{5.2}$$

As seen in Eq (4.23) the electron in the DQD couples to the microwave photons through a term which is proportional to $\widehat{N}_L$. If we want to quantitatively understand the strength of the coupling, we need to write the matrix elements of $\widehat{N}_L$ in the eigenbasis of H_{DQD}. Since the coupling elements prove to be functions of both $\frac{E_C}{t}$ and n, we visualise them in a contour plot centered at the sweet spot which is at $n = N/2 = 0.5$.

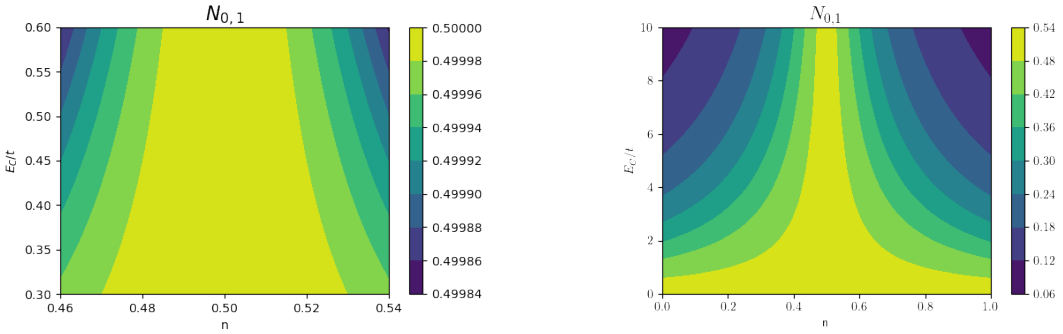

(a) (b)

Figure 5: Panel a and b show the matrix element of the coupling between the $|E_0\rangle$ and $|E_1\rangle$ qubit states: $(\langle E_0| \widehat{N}_L |E_1\rangle = N_{0,1})$ plotted against the detuning parameter n and the ratio between the charging energy and the tunneling strength. The figures show an invariance in the coupling term to the value of E_C/t along the sweet spot $n = 0.5$ where the DQD has better protection from noise. The coupling term tells us how strong the microwave photons couple to the double quantum dot.

In Figure 5, we can see that the coupling term at $n = 0.5$, where the sweet spot is, is independent of the charging energy and tunneling term to first order in n. As a consequence, it is not possible to tune the strength of the coupling term by changing $\frac{E_C}{t}$. This invariance can be seen analytically by substituting $n_g = 0.5$ into Eq. (5.2) and noting that the eigen states are then independent of $\frac{E_C}{t}$. However, the coupling strength is in fact maximized at the sweet spot ($n = 0.5$) which allows for interactions between the charge and the photons in the resonator while minimizing the influence of charge noise on the DQD. The figures also show that the coupling magnitude is more stable in the neigbourhood of $n = 1$ when $\frac{E_C}{t}$ is small. In other words, near $n = 1$, $\frac{dN}{dn}$ is small when $\frac{E_C}{t}$ is small.

5.2 Two Electrons Double Quantum Dot

We now turn our attention to the state of a DQD when the total charge is restricted to only two electrons. In this case, the state of the system is an element in the product space spanned by the basis in Eq. (2.4). In this basis, the DQD Hamiltonian Eq. (4.31) can be written in matrix form by calculating $\langle u_i | H_{DQD} | u_j \rangle$ directly, as shown in the following equation. The basis vectors are ordered according to Eq. (2.4):

$$H_{DQD} \longrightarrow \begin{bmatrix} E_c(n-1)^2 & 0 & 0 & 0 & 0 & 0 \\ 0 & E_c(n-1)^2 & 0 & 0 & t & t \\ 0 & 0 & E_c(n-1)^2 & 0 & -t & -t \\ 0 & 0 & 0 & E_c(n-1)^2 & 0 & 0 \\ 0 & t & -t & 0 & E_c(n-2)^2 & 0 \\ 0 & t & -t & 0 & 0 & E_c n^2 \end{bmatrix}. \quad (5.3)$$

Note that, without spin-orbit coupling in the DQD and since the system is assumed to be closed, the total spin of the electrons must be conserved. Here the total spin operator is defined by

$$S^2 = S_L^2 + S_R^2 + 2S_{L,z}S_{R,z} + S_{L,+}S_{R,-} + S_{L,-}S_{R_+},$$

defined by the typical spin operators for the $|L\rangle$ and $|R\rangle$ orbitals. In second quantization, these are written as:

$$\begin{aligned} S_{L,z} &= c^\dagger_{L,\uparrow}c_{L,\uparrow} - c^\dagger_{L,\downarrow}c_{L,\downarrow}, \\ S_{L,x} &= c^\dagger_{L,\uparrow}c_{L,\downarrow} + c^\dagger_{L,\downarrow}c_{L,\uparrow}, \\ S_{L,y} &= ic^\dagger_{L,\uparrow}c_{L,\downarrow} - ic^\dagger_{L,\downarrow}c_{L,\uparrow}, \\ S_{L,\pm} &= S_{L,x} \pm iS_{L,y}. \end{aligned}$$

Using these operators one can check the conservation of spin by verifying that $[\widehat{H}_{DQD}, \widehat{S}^2] = 0$, or by observing the form of H_{DQD}. Consequently, there must exist a common basis that diagonalizes both operators. With these insights in mind, we continue the calculations by first introducing the singlet-triplet basis which are eigenkets of the total spin operator $\widehat{S}^2$ and then write the DQD Hamiltonian in this basis.
Defining the singlet-triplet basis in terms of Eq. (2.4), we have:

$$
\begin{aligned}
|S_0\rangle &= \frac{1}{\sqrt{2}}(c^\dagger_{L\uparrow}c^\dagger_{R\downarrow} - c^\dagger_{L\downarrow}c^\dagger_{R\uparrow})\,|0\rangle \\
|S_+\rangle &= \frac{1}{\sqrt{2}}(c^\dagger_{L\uparrow}c^\dagger_{L\downarrow} + c^\dagger_{R\uparrow}c^\dagger_{R\downarrow})\,|0\rangle \\
|S_-\rangle &= \frac{1}{\sqrt{2}}(c^\dagger_{L\uparrow}c^\dagger_{L\downarrow} - c^\dagger_{R\uparrow}c^\dagger_{R\downarrow})\,|0\rangle \\
|T_0\rangle &= \frac{1}{\sqrt{2}}(c^\dagger_{L\uparrow}c^\dagger_{R\downarrow} + c^\dagger_{L\downarrow}c^\dagger_{R\uparrow})\,|0\rangle \\
|T_+\rangle &= \frac{1}{\sqrt{2}}(c^\dagger_{L\uparrow}c^\dagger_{R\uparrow} + c^\dagger_{L\downarrow}c^\dagger_{R\downarrow})\,|0\rangle \\
|T_-\rangle &= \frac{1}{\sqrt{2}}(c^\dagger_{L\uparrow}c^\dagger_{R\uparrow} - c^\dagger_{L\downarrow}c^\dagger_{R\downarrow})\,|0\rangle\,.
\end{aligned}
\tag{5.4}
$$

These basis are eigenstates of the total spin operator satisfying $S^2\,|S\rangle = 0$ and $S^2\,|T\rangle = 2\,|T\rangle$. The Hamiltonian matrix Eq. (5.6) can now be rotated to the singlet triplet basis by using Eq. (5.4). We obtain:

$$
H_{DQD} \longrightarrow \begin{bmatrix}
E_c(n-1)^2 & 2t & 0 & 0 & 0 & 0 \\
2t & E_c(n^2-2n+2) & 2E_c(1-n) & 0 & 0 & 0 \\
0 & 2E_c(1-n) & E_c(n^2-2n+2) & 0 & 0 & 0 \\
0 & 0 & 0 & E_c(n-1)^2 & 0 & 0 \\
0 & 0 & 0 & 0 & E_c(n-1)^2 & 0 \\
0 & 0 & 0 & 0 & 0 & E_c(n-1)^2
\end{bmatrix}.
\tag{5.5}
$$

Because the total spin operator $\widehat{S}^2$ is degenerate, the DQD Hamiltonian can be written in block diagonal form in the singlet-triplet basis. Since the conservation of spin holds and the triplet states degenerate and are therefore uninteresting, we can simplify the problem by assuming the initial state of the system to be in the singlet subspace Accordingly, the DQD in the singlet basis $\{|S_0\rangle\,, |S_+\rangle\,, |S_-\rangle\}$ (scaled by $1/t$ for simplicity), is given by:

$$
H_{S/t} = \frac{H_S}{t} = \begin{bmatrix}
\frac{E_c}{t}(n-1)^2 & 2 & 0 \\
2 & \frac{E_c}{t}(n^2-2n+2) & 2\frac{E_c}{t}(1-n) \\
0 & 2\frac{E_c}{t}(1-n) & \frac{E_c}{t}(n^2-2n+2)
\end{bmatrix}
\tag{5.6}
$$

To find the eigen energies allowed for this system we must solve for $\mathrm{Det}(H_S/t - EI) = 0$ which gives a cubic equation in E, making it hard to present the solutions in their full generality. We, therefore, restrict ourselves to numerical solutions for the eigen-energies given a specific value of E_C/t and we plot them as functions of the detuning parameter n as shown in the figure bellow.

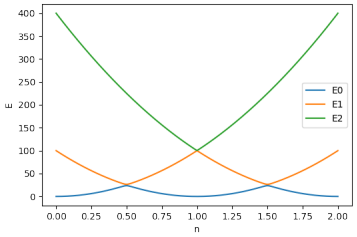

Figure 6: No tunneling limit

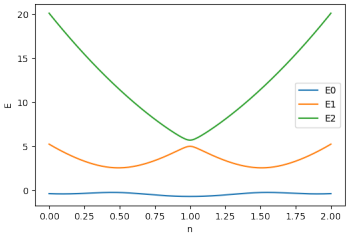

Figure 7: $E_C/t = 5$

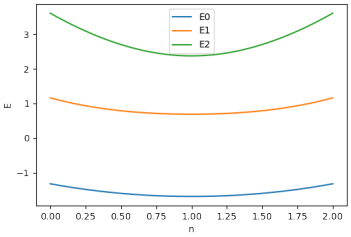

Figure 8: $E_C/t \approx 0.69$

Figure: Plots of the eigen energies of the double quantum dot. a) shows the energies in the small coupling regime where the energies charging parabolas. Three points of degeneracy occur as the tunneling term goes to zero. b) The introduction of a tunneling term lifts the degeneracy resulting in three energy levels. c) at the sweet spot $E_C/t = 0.69$ the difference between the lowest two energies is constant in the neighbourhood of $n = 1$

Figure 6 shows that when the tunneling is suppressed, only the charging energy term in Eq. (4.27) plays a role and we get three energy parabolas that correspond to two-electron singlet states where there is 0,1 or 2 electrons in the left dot. As the tunneling strength is increased Figure 7, the three degeneracy points seen in Figure 6 are lifted and their place is taken by energy gaps. Going to the sweet spot limit [14] at $E_C/t \approx 0.69$ and $n = 1$ as in Figure 8 where, we see that indeed the energy difference between the lowest two terms is insensitive to fluctuations in the detuning n. It is therefore possible to encode a qubit into this DQD system by projecting into the space spanned by the lowest two levels $|E_0\rangle$ and $|E_1\rangle$.
Turning our attention to the coupling term. We express the matrix elements of $\widehat{N}_L$ in the singlet basis by evaluating $\langle S_i| \widehat{N}_L |S_j\rangle$, where $\widehat{N}_L = C^\dagger_{L,\downarrow} C_{L,\downarrow} + C^\dagger_{L,\uparrow} C_{L,\uparrow}$ and we find:

$$\widehat{N}_L \longrightarrow \begin{bmatrix} \langle S_0| \widehat{N}_L |S_0\rangle & \langle S_0| \widehat{N}_L |S_+\rangle & \langle S_0| \widehat{N}_L |S_-\rangle \\ \langle S_+| \widehat{N}_L |S_0\rangle & \langle S_+| \widehat{N}_L |S_+\rangle & \langle S_+| \widehat{N}_L |S_-\rangle \\ \langle S_-| \widehat{N}_L |S_0\rangle & \langle S_-| \widehat{N}_L |S_+\rangle & \langle S_-| \widehat{N}_L |S_-\rangle \end{bmatrix} = \begin{bmatrix} 1 & 0 & 0 \\ 0 & 1 & 1 \\ 0 & 1 & 1 \end{bmatrix}. \tag{5.7}$$

Finally, we want to find the N_L in the singlet energy eigenbasis. However, since it is difficult to write down the eigen kets in their full generality, we will restrict ourselves to the case of interest, which is at the higher-order sweet spot which appears at $n = 1$ and $E_C/t \approx 0.69$ Given specific values of $\frac{E_C}{t}$ and n, we can numerically solve for the eigen states of the single-subspace energy eigen states and use them to find the matrix elements of N_L.

$$N_{0,1}(E_C, t, n) = \langle E_0(E_C, t, n)| \widehat{N}_L |E_1(E_C, t, n)\rangle . \tag{5.8}$$

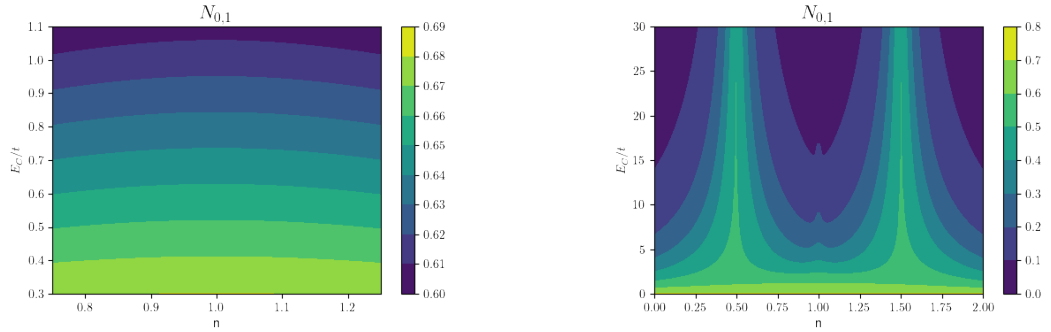

(a) (b)

Figure 9: Panel (a) and (b) show contour plots of the matrix element $\langle E_0| \widehat{N}_L |E_1\rangle$ coupling the the qubit states to the microwave photons. The figures show that at the sweet spot where the DQD is noise tolerant, the coupling to the microwave photons is non-zero and that it is tunable by changing the ratio E_C/t.

In Section 2.5, we discussed how the qubit state at the "higher-order sweet spot" ($n = 1, E_C/t \approx 0.69$) is resistant to noise and have longer coherence time. Figure 9 helps us answer the question of whether coupling to the microwave is possible at higher-order sweet spot. It shows that the coupling to microwave photons does not vanish completely, allowing for various control protocols using microwave photons. Figure 4.a shows that the strength of the coupling can be adjusted by changing the ratio of the charging energy and the tunneling term. It is worth noting that the maximum coupling strength is not achieved at the higher-order sweet spot, but can be increased by moving away from this point at the cost of reduced decoherence time.

6 Driven microwave oscillator

In this section we sketch how the coupling to the resonator allows us to control the DQD. To begin, we will consider a simplified model of the DQD qubit by only considering its lowest two energy levels. For the two electron DQD studied above, the matrix representing the coupling term N_L in the basis $\{|0\rangle, |1\rangle\}$ (the lowest two energy states) is found by using Eq. (5.7) and the two eigenstates of Eq. (5.6) at $n = 1$.

$$\widehat{N}_L \longrightarrow \begin{bmatrix} 1 & \frac{4}{\sqrt{\left(E_t+\sqrt{E_t^2+16}\right)^2+16}} \\ \frac{4}{\sqrt{\left(E_t+\sqrt{E_t^2+16}\right)^2+16}} & 1 \end{bmatrix} \tag{6.1}$$

Where we define $E_t = E_C/t$. The simplest type of control that we can apply to a qubit is to drive the microwave resonator with an oscillatory signal. Eq. (6.1) showes that N_L has no σ_z component and we can write the Hamiltonian for the full system as :

$$H = \frac{\hbar\Omega}{2}(\mathbb{1})_H \otimes (\sigma_z)_D + \hbar\omega(\mathbb{1})_D \otimes (a^\dagger a)_H + g(a + a^\dagger)_H \otimes (\sigma_x)_D, \tag{6.2}$$

where σ_x, σ_z are the Pauli matrices in the qubit basis $\{|0\rangle, |1\rangle\}$ and g is the coupling constant. Here, the subscripts H and D denote operators that are defined on the state of the bosons in the harmonic oscillator and the state of the electrons in the double quantum dot respectively. Let the microwave resonator be driven strongly at frequency ω :

$$(a + a^\dagger) \longrightarrow \left\langle a + a^\dagger \right\rangle = V(t) = V_0 \cos(\omega t) = V_0 \frac{(e^{i\omega t} + e^{-i\omega t})}{2}. \tag{6.3}$$

Substituting this into Eq (6.2), we find:

$$H = \frac{\hbar\Omega}{2}\sigma_z + \frac{gV_0}{2}\left(\left(e^{i\omega t}\sigma_- + e^{-i\omega t}\sigma_+\right) + \left(e^{-i\omega t}\sigma_- + e^{i\omega t}\sigma_+\right)\right). \tag{6.4}$$

When the resonator is driven close to resonance with qubit splitting ($\omega \approx \Omega$), the RWA can be used to eliminate certain rapidly oscillating terms, $(e^{-i\omega t}\sigma_- + e^{i\omega t}\sigma_+)$, in the Hamiltonian. This approximation is valid as long as the time scale of the system's evolution is much longer than the time scale of the fast oscillations. The semi-classical Hamiltonian, after the application of RWA, is then given.

$$H_{SC} = \frac{\Omega\hbar}{2}\sigma_z + \frac{gV_0}{2}\begin{bmatrix} 0 & e^{i\omega t} \\ e^{-i\omega t} & 0 \end{bmatrix} = \begin{bmatrix} \frac{\Omega\hbar}{2} & \frac{gV_0}{2}e^{i\omega t} \\ \frac{gV_0}{2}e^{-i\omega t} & \frac{-\Omega\hbar}{2} \end{bmatrix}. \tag{6.5}$$

Eq (6.5) is nothing but the Rabi problem which, given a state

$$|\psi\rangle = \alpha|0\rangle + \beta|1\rangle \tag{6.6}$$

that is initially in the ground state $\alpha(t=0)=1$ and $\beta(t=0)=0$, gives the following solutions [17, p.340]

$$\alpha(t) = \frac{\frac{g^2V_0^2}{4\hbar^2}}{\frac{g^2V_0^2}{4\hbar^2}+(\Omega-\omega)^2/4}\sin^2\left(\left[\frac{g^2V_0^2}{4\hbar^2}+(\Omega-\omega)^2/4\right]^{1/2}t\right)$$
$$|\beta(t)|^2 = 1-|\alpha(t)|^2.$$

When in resonance, the qubit oscillates between the two states at frequency $\omega_R = \frac{gV_0}{2}$. Where for a DQD with two electrons the coupling g is given by

$$g \propto N_{L(0,1)} = \frac{4}{\sqrt{(\frac{E_C}{t}-\sqrt{\left(\frac{E_C}{t}\right)^2+16})^2+16}}. \tag{6.7}$$

Thus, by driving the microwave resonator, one could control the state of the DQD qubit. Furthermore, the frequency of the Rabi oscillations are determined by the strength of the coupling term and can therefore by tuned to a specific value by changing $\frac{E_c}{t}$ as seen in Eq. (6.7).

7 Conclusion

In conclusion, we have combined methods from electrostatics and cQED to provide an original derivation of the Hamiltonian describing the dynamics of dobule quantum dot in a microwave resonator. We found that the coupling to the microwave resonator is possible when the double quantum dot is operated in the higher-order sweet spot. Additionally, we demonstrated that both the Rabi frequency in the case of strong oscillator drive and the coupling to the microwave frequency can be tuned by adjusting the charging energy and the tunneling constant of the DQD. These findings provide a foundation for further investigation into the potential use of DQDs in quantum computing.

8 Outlook

In this study, we derived an expression that provides a foundation for investigating the dynamics and time evolution of the interaction between double quantum dots (DQDs) and microwave photons. To accurately model these systems, we must further consider the effects of the surrounding environment and other factors such as spin-orbit interactions and higher excitation modes of the resonator. Our findings suggest that DQDs are a promising candidate for use in quantum computing due to their enhanced coherence time at the higher-order sweet spot and the ability to couple to microwave photons. Further experiments are needed to confirm this potential benefit. This research is relevant to the fields of circuit quantum electrodynamics, quantum sensing, light-matter interactions, hybrid quantum circuits, and quantum information and its implementation.

References

[1] Alexander Altland and Ben Simons. *Condensed matter field theory. [Elektronisk resurs].* Cambridge University Press, 2010. ISBN: 9780521769754. URL: https://ludwig.lub.lu.se/login?url=https://search.ebscohost.com/login.aspx?direct=true&AuthType=ip,uid&db=cat07147a&AN=lub.6053294&site=eds-live&scope=site.

[2] Alexandre Blais et al. "Circuit Quantum Electrodynamics." In: (2020). URL: https://ludwig.lub.lu.se/login?url=https://search.ebscohost.com/login.aspx?direct=true&AuthType=ip,uid&db=edsarx&AN=edsarx.2005.12667&site=eds-live&scope=site.

[3] Alexandre Blais et al. "Circuit Quantum Electrodynamics." In: (2020). URL: https://ludwig.lub.lu.se/login?url=https://search.ebscohost.com/login.aspx?direct=true&AuthType=ip,uid&db=edsarx&AN=edsarx.2005.12667&site=eds-live&scope=site.

[4] A. A. Clerk et al. "Hybrid quantum systems with circuit quantum electrodynamics." In: *Nature Physics* 16.3 (2020), pp. 257–267. ISSN: 1745-2473. URL: https://ludwig.lub.lu.se/login?url=https://search.ebscohost.com/login.aspx?direct=true&AuthType=ip,uid&db=edssjs&AN=edssjs.A73C4D94&site=eds-live&scope=site.

[5] A.A. Clerk et al. "Hybrid quantum systems with circuit quantum electrodynamics." In: *Nature Physics* 16.3 (2020), pp. 257–267. URL: https://ludwig.lub.lu.se/login?url=https://search.ebscohost.com/login.aspx?direct=true&AuthType=ip,uid&db=inh&AN=20605453&site=eds-live&scope=site.

[6] Michel H Devoret et al. "Quantum fluctuations in electrical circuits". In: *Les Houches, Session LXIII* 7.8 (1995), pp. 133–135.

[7] Michel H. Devoret and John M. Martinis. "Implementing Qubits with Superconducting Integrated Circuits." In: *Quantum Information Processing* 3.1-5 (2004), pp. 163–203. ISSN: 15700755. URL: https://ludwig.lub.lu.se/login?url=https://search.ebscohost.com/login.aspx?direct=true&AuthType=ip,uid&db=a9h&AN=20925137&site=eds-live&scope=site.

[8] Michel H. Devoret and John M. Martinis. "Implementing Qubits with Superconducting Integrated Circuits." In: *Quantum Information Processing* 3.1-5 (2004), pp. 163–203. ISSN: 15700755. URL: https://ludwig.lub.lu.se/login?url=https://search.ebscohost.com/login.aspx?direct=true&AuthType=ip,uid&db=a9h&AN=20925137&site=eds-live&scope=site.

[9] S. M. Girvin. *Circuit QED: superconducting qubits coupled to microwave photons.* Oxford University Press, 2014. ISBN: 978-0-19-176145-4. URL: https://ludwig.lub.lu.se/login?url=https://search.ebscohost.com/login.aspx?direct=true&AuthType=ip,uid&db=edsoso&AN=edsoso.9780199681181.003.0003&site=eds-live&scope=site.

[10] R. Hanson et al. "Spins in few-electron quantum dots". In: *Rev. Mod. Phys.* 79 (4 Oct. 2007), pp. 1217–1265. DOI: 10.1103/RevModPhys.79.1217. URL: https://link.aps.org/doi/10.1103/RevModPhys.79.1217.

[11] Shannon Harvey. "Quantum Dots / Spin Qubits." In: (2022). URL: https://ludwig.lub.lu.se/login?url=https://search.ebscohost.com/login.aspx?direct=true&AuthType=ip,uid&db=edsarx&AN=edsarx.2204.04261&site=eds-live&scope=site.

[12] G. Ithier et al. "Decoherence in a superconducting quantum bit circuit." In: (2005). URL: https://ludwig.lub.lu.se/login?url=https://search.ebscohost.com/login.aspx?direct=true&AuthType=ip,uid&db=edsarx&AN=edsarx.cond-mat%2f0508588&site=eds-live&scope=site.

[13] Waqar Khan et al. "Efficient and continuous microwave photoconversion in hybrid cavity-semiconductor nanowire double quantum dot diodes." In: *Nature Communications NanoLund: Center for Nanoscience* 12.1 (2021). ISSN: 2041-1723. URL: https://ludwig.lub.lu.se/login?url=https://search.ebscohost.com/login.aspx?direct=true&AuthType=ip,uid&db=edsswe&AN=edsswe.oai.lup.lub.lu.se.3f7ec643.7d31.4abe.8a98.935c2ae1df20&site=eds-live&scope=site.

[14] Morten I. K. Munk et al. "Coherence improvements in double quantum dots with higher-order sweet spot." In: *In preparation* ().

[15] Michael A. Nielsen and Isaac L. Chuang. *Quantum computation and quantum information.* Cambridge University Press, 2010. ISBN: 9781107002173. URL: https://ludwig.lub.lu.se/login?url=https://search.ebscohost.com/login.aspx?direct=true&AuthType=ip,uid&db=cat07147a&AN=lub.1981523&site=eds-live&scope=site.

[16] Carlos Outeiral et al. "The prospects of quantum computing in computational molecular biology." In: (2020). URL: https://ludwig.lub.lu.se/login?url=https://search.ebscohost.com/login.aspx?direct=true&AuthType=ip,uid&db=edsarx&AN=edsarx.2005.12792&site=eds-live&scope=site.

[17] Jun John Sakurai and Jim Napolitano. *Modern quantum mechanics.* Cambridge University Press, 2017. ISBN: 9781108422413. URL: https://ludwig.lub.lu.se/login?url=https://search.ebscohost.com/login.aspx?direct=true&AuthType=ip,uid&db=cat07147a&AN=lub.7082833&site=eds-live&scope=site.

[18] Jérémie J. Viennot et al. "Towards hybrid circuit quantum electrodynamics with quantum dots." In: *Comptes rendus - Physique* 17.7 (2016), pp. 705–717. ISSN: 1631-0705. URL: https://ludwig.lub.lu.se/login?url=https://search.ebscohost.com/login.aspx?direct=true&AuthType=ip,uid&db=edselp&AN=S1631070516300597&site=eds-live&scope=site.

Appendix

A list of the constants defined in this text

The capacitance matrix of the circuit in figure (4), was found to be:

$$\vec{C} = \begin{bmatrix} C_L + C + C_R & -C_R & -C_L \\ -C_R & C_C + C_R + C_{gR} & -C_C \\ -C_L & -C_C & C_C + C_L + C_{gL} \end{bmatrix}$$

In section 4.2) the following definitions were made:

$$\begin{aligned} \alpha_n &= M_{1,1} \\ \alpha_L &= M_{3,3} \\ \alpha_R &= M_{2,2} \\ \beta_n &= C_{gL}V_L M_{1,3} + C_{gR}V_R M_{1,2} \\ \beta_L &= C_{gL}V_L M_{3,3} + C_{gR}V_R M_{2,3} \\ \beta_R &= C_{gL}V_L M_{2,3} + C_{gR}V_R M_{2,2} \\ \gamma_L &= M_{1,3} \\ \gamma_R &= M_{1,2} \\ \delta &= M_{2,3} \end{aligned}$$

,where M is the inverse of the capacitance matrix.
From section 4.4:

$$\omega_Q = e \cdot \gamma_-(4\hbar^2 L\alpha_n)^{-1/4}$$
$$\omega_o = \left(\beta_n + e\frac{N}{2}\gamma_+ - e\frac{N}{2}\gamma_-\right)\left(4\hbar^2 L\alpha_n\right)^{-1/4}$$
$$\beta_L^{'} = \beta_L - \left(\frac{2\hbar\omega_Q\omega_o}{e\omega}\right)$$

Solutions to the system of equations in section 4.5

$$k = \sqrt{\frac{(\alpha_L - \delta)}{(\alpha_R - \delta)}}$$

$$B = (\frac{\alpha_L - \delta}{2})(\frac{1}{1+k^2}) = (\frac{\alpha_L - \delta}{2})(\frac{(\alpha_R - \delta)}{\alpha_L + \alpha_R - 2\delta})$$

$$A = B + \frac{\delta}{2} = \frac{(\alpha_R - \delta)(\alpha_L - \delta) + \delta(\alpha_L + \alpha_R - 2\delta)}{2(\alpha_L + \alpha_R - 2\delta)}$$

$$n_g = \frac{\beta_R - \beta_L^{'}}{\sqrt{(\alpha_R - \delta)(\alpha_L - \delta)}}$$
$$N_g = \frac{\beta_L^{'} + k^2\beta_R}{-2(1+k^2)A} = \frac{\beta_L^{'} + \frac{(\alpha_L - \delta)}{(\alpha_R - \delta)}\beta_R}{-2(1 + \frac{(\alpha_L - \delta)}{(\alpha_R - \delta)})\frac{(\alpha_R - \delta)(\alpha_L - \delta) + \delta(\alpha_L + \alpha_R - 2\delta)}{2(\alpha_L + \alpha_R - 2\delta)}}$$

Finally in section 4.5 we defined:

$$E_C = Be^2(k + \frac{1}{k})^2, \tag{8.1}$$
$$n = \frac{\frac{n_g}{e} + \frac{N}{k}}{k + \frac{1}{k}}. \tag{8.2}$$

An LC circuit in series with two capacitors (an illustrative example)

Consider a circuit where we have an LC oscillator with capacitance C_1 and inductance L connected in series to two other capacitors C_2 and C_3. Furthermore, let the left plate of C_3 be held to voltage V as shown in figure (10).

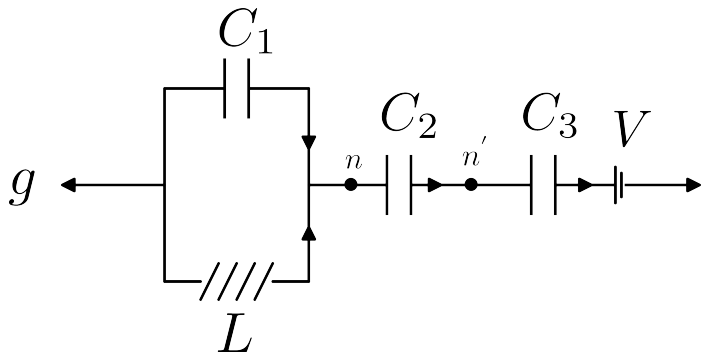

Figure 10: A circuit diagram for an LC resonator in parallel with two capacitors C_2 and C_3. This circuit can be used as a model for a quantum dot placed at node n' and is coupled to a mode of the microwave resonator (a photon) with frequency equal to that of the LC resonator seen to the left of the circuit.

Following our algorithm mentioned above we assign node fluxes to n and n' and use them to express branch currents with the help of eq (3.7) and eq (3.6).

$$i_{C_1} = \frac{dQ_b}{dt} = \frac{\dot{V}_{C_1}}{C_1} = \frac{\ddot{\phi}_n}{C_1} \tag{8.3}$$

$$i_{C_2} = \dot{Q}_{C_2} = \frac{\ddot{\phi}_n' - \ddot{\phi}_n}{C_2} \tag{8.4}$$

$$i_{C_3} = \dot{V} - \ddot{\phi}_n{}' \tag{8.5}$$

$$i_L = \frac{\phi_n}{L} \tag{8.6}$$

we now use these expressions to write Kirchhoff's current law (KCL) eq(3.2)) for each of the nodes

$$C_1\ddot{\phi}_n + \frac{\phi_n}{L} = C_2(\ddot{\phi}_{n'} - \ddot{\phi}_n) \tag{8.7}$$

$$C_2(\ddot{\phi}_{n'} - \ddot{\phi}_n) = C_3(\dot{V} - \ddot{\phi}_{n'})$$

These differential equations can be shown to be the Euler-Lagrange equations of the following Lagrangian:

$$\mathcal{L} = \frac{C_1}{2}\dot{\phi}_n^2 + \frac{C_2}{2}(\dot{\phi}_{n'} - \dot{\phi}_n)^2 + \frac{C_3}{2}(V - \dot{\phi}_{n'})^2 - \frac{\phi_n^2}{2L}$$

Comparing with eq (3.8-3.9) we see that the Lagrangian is given by the energy difference between the capacitive and inductive elements. That is, the dynamics of the system is dictated by the interplay between the energy stored in the electric field of the capacitors and the energy stored in the magnetic field of the inductor. To perform a Legendre transformation

we define the generalised conjugate momenta:

$$Q_n = \frac{d\mathcal{L}}{d\dot{\phi}_n} = (C_1 + C_2)\dot{\phi}_n - C_2\dot{\phi}_{n'} \tag{8.8}$$

$$Q_{n'} = \frac{d\mathcal{L}}{d\dot{\phi}_{n'}} = -C_2\dot{\phi}_n + (C_2 + C_3)\dot{\phi}_{n'} - C_3V \tag{8.9}$$

We see that these conjugate momenta Q represent the charge residing on the nodes. This can easily be seen in

$$Q_{n'} = C_2(\dot{\phi}_{n'} - \dot{\phi}_n) - C_3(V - \dot{\phi}_{n'}) = Q_{C_2} - Q_{C_3}$$

where Q_{C_2} and Q_{C_3} are the charges on plates of the capacitors C_2 and C_3. This is a very important feature of our circuit model. The dynamical variables describing our system are directly related to the charge residing on the nodes. This allows us to think of the momentum $Q_n^{'}$ as the charge on the Quantum dot placed at node $n^{'}$.
Casting these relations (8.9) into matrix form, one obtains

$$\begin{bmatrix} Q_n \\ Q_{n'} + C_3V \end{bmatrix} = \begin{bmatrix} C_1 + C_2 & -C_2 \\ -C_2 & C_2 + C_3 \end{bmatrix} \cdot \begin{bmatrix} \dot{\phi}_n \\ \dot{\phi}_{n'} \end{bmatrix} \tag{8.10}$$

It is also useful to write the inverse of this expression:

$$\begin{bmatrix} \dot{\phi}_n \\ \dot{\phi}_{n'} \end{bmatrix} = \frac{1}{D}\begin{bmatrix} C_2 + C_3 & C_2 \\ C_2 & C_1 + C_2 \end{bmatrix} \cdot \begin{bmatrix} Q_n \\ Q_{n'} + C_3V \end{bmatrix} \tag{8.11}$$

where $D = det(\vec{C}) = C_1C_2 + C_1C_3 + C_2C_3$.

The Legendre transform of our Lagrangian is then given by:

$$H = Q_n\dot{\phi}_n + Qn^{'}\dot{\phi}n^{'} - \mathcal{L} \tag{8.12}$$

$$= \frac{Q_n\dot{\phi}_n}{2} + \frac{(Q_{n'} + C_3V)\dot{\phi}_{n'}}{2} + \frac{\phi_n^2}{2L} \tag{8.13}$$

$$= \frac{1}{2}\left[\dot{\phi}_n, \dot{\phi}_{n'}\right] \cdot \begin{bmatrix} Q_n \\ Q_{n'} + C_3V \end{bmatrix} + \frac{\phi_n^2}{2L} \tag{8.14}$$

Finally we completer our transformation by using eq (8.11) to get the Hamiltonian

$$H = \frac{1}{2}\begin{bmatrix} Q_n & Q_{n'} + C_3V \end{bmatrix} \cdot (C^{-1})^T \cdot \begin{bmatrix} Q_n \\ Q_{n'} + C_3V \end{bmatrix} + \frac{\phi_n^2}{2L} \tag{8.15}$$

expanded

$$H = \frac{(C_2 + C_3)}{2D}Q_n^2 + \frac{C_2(Q_{n'} + C_3V)}{D}Q_n + \frac{(C_1 + C_2)}{2D}(C_3V + Q_{n'})^2 + \frac{\phi_n^2}{2L}.$$